International Telecommunication Union

ITU-R

Radiocommunication Sector of ITU

Recommendation ITU-R P.618-12

(07/2015)

Propagation data and prediction methods required for the design of Earth-space telecommunication systems

P Series

Radiowave propagation

Foreword

The role of the Radiocommunication Sector is to ensure the rational, equitable, efficient and economical use of the radio-frequency spectrum by all radiocommunication services, including satellite services, and carry out studies without limit of frequency range on the basis of which Recommendations are adopted.

The regulatory and policy functions of the Radiocommunication Sector are performed by World and Regional Radiocommunication Conferences and Radiocommunication Assemblies supported by Study Groups.

Policy on Intellectual Property Right (IPR)

ITU-R policy on IPR is described in the Common Patent Policy for ITU-T/ITU-R/ISO/IEC referenced in Annex 1 of Resolution ITU-R 1. Forms to be used for the submission of patent statements and licensing declarations by patent holders are available from http://www.itu.int/ITU-R/go/patents/en where the Guidelines for Implementation of the Common Patent Policy for ITU-T/ITU-R/ISO/IEC and the ITU-R patent information database can also be found.

Series of ITU-R Recommendations

(Also available online at http://www.itu.int/publ/R-REC/en)

Series	Title
BO	Satellite delivery
BR	Recording for production, archival and play-out; film for television
BS	Broadcasting service (sound)
BT	Broadcasting service (television)
F	Fixed service
M	Mobile, radiodetermination, amateur and related satellite services
P	**Radiowave propagation**
RA	Radio astronomy
RS	Remote sensing systems
S	Fixed-satellite service
SA	Space applications and meteorology
SF	Frequency sharing and coordination between fixed-satellite and fixed service systems
SM	Spectrum management
SNG	Satellite news gathering
TF	Time signals and frequency standards emissions
V	Vocabulary and related subjects

Note: *This ITU-R Recommendation was approved in English under the procedure detailed in Resolution ITU-R 1.*

Electronic Publication
Geneva, 2015

RECOMMENDATION ITU-R P.618-12*

Propagation data and prediction methods required for the design of Earth-space telecommunication systems

(Question ITU-R 206/3)

(1986-1990-1992-1994-1995-1997-1999-2001-2003-2007-2009-2013-2015)

Scope

This Recommendation predicts the various propagation parameters needed in planning Earth-space systems operating in either the Earth-to-space or space-to-Earth direction.

The ITU Radiocommunication Assembly,

considering

a) that for the proper planning of Earth-space systems, it is necessary to have appropriate propagation data and prediction techniques;

b) that methods have been developed that allow the prediction of the most important propagation parameters needed in planning Earth-space systems;

c) that as far as possible, these methods have been tested against available data and have been shown to yield an accuracy that is both compatible with the natural variability of propagation phenomena and adequate for most present applications in system planning,

recommends

that the methods for predicting the propagation parameters set out in Annex 1 should be adopted for planning Earth-space radiocommunication systems, in the respective ranges of validity indicated in Annex 1.

NOTE 1 – Supplementary information related to the planning of broadcasting-satellite systems as well as maritime, land, and aeronautical mobile-satellite systems, may be found in Recommendations ITU-R P.679, ITU-R P.680, ITU-R P.681 and ITU-R P.682, respectively.

* Radiocommunication Study Group 3 made editorial amendments to this Recommendation in 2016 in accordance with Resolution ITU-R 1.

Annex 1

1 Introduction

In the design of Earth-space links for communication systems, several effects must be considered. Effects of the non-ionized atmosphere need to be considered at all frequencies, but become critical above about 1 GHz and for low elevation angles. These effects include:

a) absorption in atmospheric gases; absorption, scattering and depolarization by hydrometeors (water and ice droplets in precipitation, clouds, etc.); and emission noise from absorbing media; all of which are especially important at frequencies above about 10 GHz;

b) loss of signal due to beam-divergence of the earth-station antenna, due to the normal refraction in the atmosphere;

c) a decrease in effective antenna gain, due to phase decorrelation across the antenna aperture, caused by irregularities in the refractive-index structure;

d) relatively slow fading due to beam-bending caused by large-scale changes in refractive index; more rapid fading (scintillation) and variations in angle of arrival, due to small-scale variations in refractive index;

e) possible limitations in bandwidth due to multiple scattering or multipath effects, especially in high-capacity digital systems;

f) attenuation by the local environment of the ground terminal (buildings, trees, etc.);

g) short-term variations of the ratio of attenuations at the up- and down-link frequencies, which may affect the accuracy of adaptive fade countermeasures;

h) for non-geostationary satellite (non-GSO) systems, the effect of varying elevation angle to the satellite.

Ionospheric effects (see Recommendation ITU-R P.531) may be important, particularly at frequencies below 1 GHz. For convenience these have been quantified for frequencies of 0.1; 0.25; 0.5; 1; 3 and 10 GHz in Table 1 for a high value of total electron content (TEC). The effects include:

j) Faraday rotation: a linearly polarized wave propagating through the ionosphere undergoes a progressive rotation of the plane of polarization;

k) dispersion, which results in a differential time delay across the bandwidth of the transmitted signal;

l) excess time delay;

m) ionospheric scintillation: inhomogeneities of electron density in the ionosphere cause refractive focusing or defocusing of radio waves and lead to amplitude fluctuations termed scintillations. Ionospheric scintillation is maximum near the geomagnetic equator and smallest in the mid-latitude regions. The auroral zones are also regions of large scintillation. Strong scintillation is Rayleigh distributed in amplitude; weaker scintillation is nearly log-normal. These fluctuations decrease with increasing frequency and depend upon path geometry, location, season, solar activity and local time. Table 2 tabulates fade depth data for VHF and UHF in mid-latitudes, based on data in Recommendation ITU-R P.531.

Accompanying the amplitude fluctuation is also a phase fluctuation. The spectral density of the phase fluctuation is proportional to $1/f^3$, where f is the Fourier frequency of the fluctuation. This spectral characteristic is similar to that arising from flicker of frequency in oscillators and can cause significant degradation to the performance of receiver hardware.

TABLE 1

Estimated* ionospheric effects for elevation angles of about 30° one-way traversal**
(derived from Recommendation ITU-R P.531)

Effect	Frequency dependence	0.1 GHz	0.25 GHz	0.5 GHz	1 GHz	3 GHz	10 GHz
Faraday rotation	$1/f^2$	30 rotations	4.8 rotations	1.2 rotations	108°	12°	1.1°
Propagation delay	$1/f^2$	25 μs	4 μs	1 μs	0.25 μs	0.028 μs	0.0025 μs
Refraction	$1/f^2$	< 1°	< 0.16°	< 2.4′	< 0.6′	< 4.2″	< 0.36″
Variation in the direction of arrival (r.m.s.)	$1/f^2$	20′	3.2′	48″	12″	1.32″	0.12″
Absorption (auroral and/or polar cap)	$\approx 1/f^2$	5 dB	0.8 dB	0.2 dB	0.05 dB	6×10^{-3} dB	5×10^{-4} dB
Absorption (mid-latitude)	$1/f^2$	< 1 dB	< 0.16 dB	< 0.04 dB	< 0.01 dB	< 0.001 dB	$< 1 \times 10^{-4}$ dB
Dispersion	$1/f^3$	0.4 ps/Hz	0.026 ps/Hz	0.0032 ps/Hz	0.0004 ps/Hz	1.5×10^{-5} ps/Hz	4×10^{-7} ps/Hz
Scintillation(1)	See Rec. ITU-R P.531	See Rec. ITU-R P.531	See Rec. ITU-R P.531	See Rec. ITU-R P.531	> 20 dB peak-to-peak	≈ 10 dB peak-to-peak	≈ 4 dB peak-to-peak

* This estimate is based on a TEC of 10^{18} electrons/m^2, which is a high value of TEC encountered at low latitudes in daytime with high solar activity.

** Ionospheric effects above 10 GHz are negligible.

(1) Values observed near the geomagnetic equator during the early night-time hours (local time) at equinox under conditions of high sunspot number.

TABLE 2

Distribution of mid-latitude fade depths due to ionospheric scintillation (dB)

Percentage of time (%)	Frequency (GHz)			
	0.1	**0.2**	**0.5**	**1**
1	5.9	1.5	0.2	0.1
0.5	9.3	2.3	0.4	0.1
0.2	16.6	4.2	0.7	0.2
0.1	25	6.2	1	0.3

This Annex deals only with the effects of the troposphere on the wanted signal in relation to system planning. Interference aspects are treated in separate Recommendations:

– interference between earth stations and terrestrial stations (Recommendation ITU-R P.452);

– interference from and to space stations (Recommendation ITU-R P.619);

– bidirectional coordination of earth stations (Recommendation ITU-R P.1412).

An apparent exception is path depolarization which, although of concern only from the standpoint of interference (e.g. between orthogonally-polarized signal transmissions), is directly related to the propagation impairments of the co-polarized direct signal.

The information is arranged according to the link parameters to be considered in actual system planning, rather than according to the physical phenomena causing the different effects. As far as possible, simple prediction methods covering practical applications are provided, along with indications of their range of validity. These relatively simple methods yield satisfactory results in most practical applications, despite the large variability (from year to year and from location to location) of propagation conditions.

As far as possible, the prediction methods in this Annex have been tested against measured data from the data banks of Radiocommunication Study Group 3 (see Recommendation ITU-R P.311).

2 Propagation loss

The propagation loss on an Earth-space path, relative to the free-space loss, is the sum of different contributions as follows:

– attenuation by atmospheric gases;

– attenuation by rain, other precipitation and clouds;

– focusing and defocusing;

– decrease in antenna gain due to wave-front incoherence;

– scintillation and multipath effects;

– attenuation by sand and dust storms.

Each of these contributions has its own characteristics as a function of frequency, geographic location and elevation angle. As a rule, at elevation angles above 10°, only gaseous attenuation, rain and cloud attenuation and possibly scintillation will be significant, depending on propagation conditions. For non-GSO systems, the variation in elevation angle should be included in the calculations, as described in § 8.

(In certain climatic zones, snow and ice accumulations on the surfaces of antenna reflectors and feeds can produce prolonged periods with severe attenuation, which might dominate even the annual cumulative distribution of attenuation.)

2.1 Attenuation due to atmospheric gases

Attenuation by atmospheric gases which is entirely caused by absorption depends mainly on frequency, elevation angle, altitude above sea level and water vapour density (absolute humidity). At frequencies below 10 GHz, it may normally be neglected. Its importance increases with frequency above 10 GHz, especially for low elevation angles. Annex 1 of Recommendation ITU-R P.676 gives a complete method for calculating gaseous attenuation, while Annex 2 of the same Recommendation gives an approximate method for frequencies up to 350 GHz.

At a given frequency the oxygen contribution to atmospheric absorption is relatively constant. However, both water vapour density and its vertical profile are quite variable. Typically, the maximum gaseous attenuation occurs during the season of maximum rainfall (see Recommendation ITU-R P.836).

2.2 Attenuation by precipitation and clouds

2.2.1 Prediction of attenuation statistics for an average year

The general method to predict attenuation due to precipitation and clouds along a slant propagation path is presented in § 2.2.1.1. The method to predict the probability of non-zero rain attenuation along a slant path is described in § 2.2.1.2.

If reliable long-term statistical attenuation data are available that were measured at an elevation angle and a frequency (or frequencies) different from those for which a prediction is needed, it is often preferable to scale these data to the elevation angle and frequency in question rather than using the general method. The recommended frequency-scaling method is found in § 2.2.1.3.

Site diversity effects may be estimated with the method of § 2.2.4.

2.2.1.1 Calculation of long-term rain attenuation statistics from point rainfall rate

The following procedure provides estimates of the long-term statistics of the slant-path rain attenuation at a given location for frequencies up to 55 GHz. The following parameters are required:

$R_{0.01}$: point rainfall rate for the location for 0.01% of an average year (mm/h)

h_s: height above mean sea level of the earth station (km)

θ: elevation angle (degrees)

φ: latitude of the earth station (degrees)

f: frequency (GHz)

R_e: effective radius of the Earth (8 500 km).

If local data for the earth station height above mean sea level is not available, an estimate can be obtained from the maps of topographic altitude given in Recommendation ITU-R P.1511.

The geometry is illustrated in Fig. 1.

FIGURE 1

Schematic presentation of an Earth-space path giving the parameters to be input into the attenuation prediction process

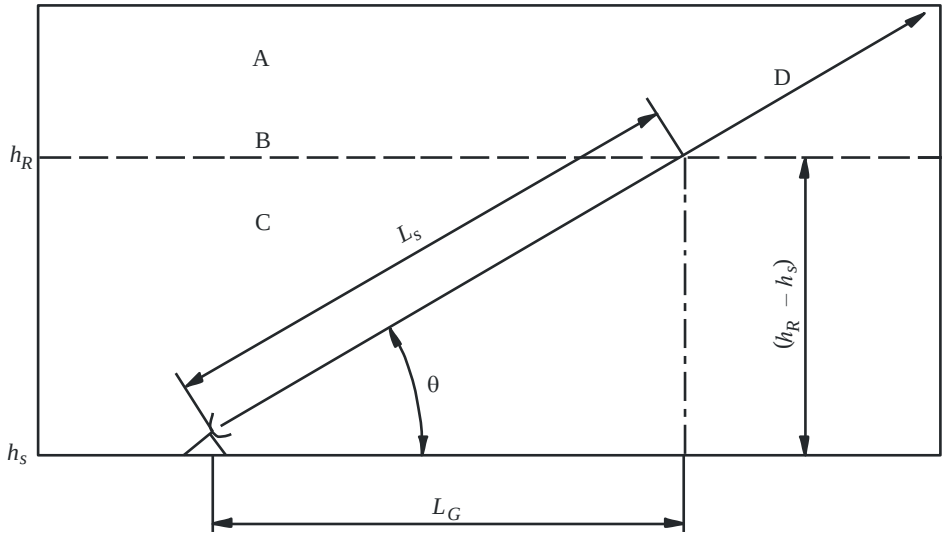

A: frozen precipitation
B: rain height
C: liquid precipitation
D: Earth-space path

P.0618-01

Step 1: Determine the rain height, h_R, as given in Recommendation ITU-R P.839.

Step 2: For $\theta \geq 5°$ compute the slant-path length, L_s, below the rain height from:

$$L_s = \frac{(h_R - h_s)}{\sin\theta} \quad \text{km} \tag{1}$$

For $\theta < 5°$, the following formula is used:

$$L_s = \frac{2(h_R - h_s)}{\left(\sin^2\theta + \frac{2(h_R - h_s)}{R_e}\right)^{1/2} + \sin\theta} \quad \text{km} \tag{2}$$

If $h_R - h_s$ is less than or equal to zero, the predicted rain attenuation for any time percentage is zero and the following steps are not required.

Step 3: Calculate the horizontal projection, L_G, of the slant-path length from:

$$L_G = L_s \cos\theta \quad \text{km} \tag{3}$$

Step 4: Obtain the rainfall rate, $R_{0.01}$, exceeded for 0.01% of an average year (with an integration time of 1 min). If this long-term statistic cannot be obtained from local data sources, an estimate can be obtained from the maps of rainfall rate given in Recommendation ITU-R P.837. If $R_{0.01}$ is equal to zero, the predicted rain attenuation is zero for any time percentage and the following steps are not required.

Step 5: Obtain the specific attenuation, γ_R, using the frequency-dependent coefficients given in Recommendation ITU-R P.838 and the rainfall rate, $R_{0.01}$, determined from Step 4, by using:

$$\gamma_R = k\,(R_{0.01})^{\alpha} \quad \text{dB/km} \tag{4}$$

Step 6: Calculate the horizontal reduction factor, $r_{0.01}$, for 0.01% of the time:

$$r_{0.01} = \frac{1}{1 + 0.78\sqrt{\frac{L_G\ \gamma_R}{f}} - 0.38\left(1 - e^{-2L_G}\right)} \tag{5}$$

Step 7: Calculate the vertical adjustment factor, $v_{0.01}$, for 0.01% of the time:

$$\zeta = \tan^{-1}\left(\frac{h_R - h_s}{L_G\ r_{0.01}}\right) \quad \text{degrees}$$

For $\zeta > \theta$, $$L_R = \frac{L_G\ r_{0.01}}{\cos\theta} \quad \text{km}$$

Else, $$L_R = \frac{(h_R - h_s)}{\sin\theta} \quad \text{km}$$

If $|\varphi| < 36°$, $$\chi = 36 - |\varphi| \quad \text{degrees}$$

Else, $$\chi = 0 \quad \text{degrees}$$

$$\nu_{0.01} = \frac{1}{1 + \sqrt{\sin\theta}\left(31\left(1 - e^{-(\theta/(1+\chi))}\right)\frac{\sqrt{L_R\ \gamma_R}}{f^2} - 0.45\right)}$$

Step 8: The effective path length is:

$$L_E = L_R\,\nu_{0.01} \quad \text{km} \tag{6}$$

Step 9: The predicted attenuation exceeded for 0.01% of an average year is obtained from:

$$A_{0.01} = \gamma_R\,L_E \quad \text{dB} \tag{7}$$

Step 10: The estimated attenuation to be exceeded for other percentages of an average year, in the range 0.001% to 5%, is determined from the attenuation to be exceeded for 0.01% for an average year:

If $p \geq 1\%$ or $|\varphi| \geq 36°$: $\beta = 0$

If $p < 1\%$ and $|\varphi| < 36°$ and $\theta \geq 25°$: $\beta = -0.005(|\varphi| - 36)$

Otherwise: $\beta = -0.005(|\varphi| - 36) + 1.8 - 4.25\sin\theta$

$$A_p = A_{0.01}\left(\frac{p}{0.01}\right)^{-(0.655 + 0.033\ln(p) - 0.045\ln(A_{0.01}) - \beta(1-p)\sin\theta)} \quad \text{dB} \tag{8}$$

This method provides an estimate of the long-term statistics of attenuation due to rain. When comparing measured statistics with the prediction, allowance should be given for the rather large year-to-year variability in rainfall rate statistics (see Recommendation ITU-R P.678).

2.2.1.2 Probability of rain attenuation on a slant path

The following procedure computes the probability of non-zero rain attenuation on a given slant path P ($A > 0$). It relies on the following input parameters:

$P_0(Lat, Lon)$: probability of rain at the earth station, ($0 \leq P_0 \leq 1$)

θ: elevation angle (degrees)

L_S: slant path length from the earth station to the rain height (km).

Step 1: Estimate the probability of rain, $P_0(Lat, Lon)$, at the earth station either from Recommendation ITU-R P.837 or from local measured rainfall rate data.

Step 2: Calculate the parameter α:

$$\alpha = Q^{-1}(P_0), \tag{9}$$

where:

$$Q(x) = \frac{1}{\sqrt{2\pi}} \int_x^{\infty} e^{-\frac{t^2}{2}} dt \tag{10}$$

Step 3: Calculate the spatial correlation function, ρ:

$$\rho = 0.59 e^{-\frac{|d|}{31}} + 0.41 e^{-\frac{|d|}{800}}, \tag{11}$$

where:

$$d = L_S . \cos\theta \tag{12}$$

and L_s is calculated in equation (2).

Step 4: Calculate the complementary bivariate normal distribution, c_B[1]:

$$c_B = \frac{1}{2\pi\sqrt{1-\rho^2}} \int_{\alpha}^{\infty} \int_{\alpha}^{\infty} e^{-\frac{x^2 - 2\rho xy + y^2}{2(1-\rho^2)}} dxdy \tag{13}$$

Step 5: Calculate the probability of rain attenuation on the slant path:

$$P(A>0) = 1 - (1 - P_0) \cdot \left(\frac{c_B - P_0^2}{P_0 (1 - P_0)} \right)^{P_0} \tag{14}$$

2.2.1.3 Long-term frequency and polarization scaling of rain attenuation statistics

Frequency scaling is the prediction of a propagation effect (e.g. rain attenuation) at one frequency from knowledge of the propagation effect at a different frequency. Typically, the frequency of the predicted propagation effect is higher than the frequency of the known propagation effect. The ratio

---

[1] NOTE – c_B is the same bivariate normal integral used in § 2.2.4.1. An approximation to this integral is available in Z. Drezner and G.O. Wesolowsky. "On the Computation of the Bivariate Normal Integral", Journal of Statistical Computation and Simulation. Vol. 35, 1989, pp. 101–107.

The Matlab statistics toolbox contains the built-in Matlab function '*mvncdf*' that computes the bivariate normal integral, and the Python library contains the built-in function 'mvndst' that computes the bivariate normal integral.

between the rain attenuation at the two frequencies can vary during a rain event, and the variability of the ratio generally increases as the rain attenuation increases.

Two prediction methods are provided in the following paragraphs:

1) Section 2.2.1.3.1 provides a method of predicting the statistical variation of the rain attenuation at frequency f_2 conditioned on the rain attenuation at frequency f_1. This method requires the cumulative distributions of rain attenuation at both frequencies.

2) Section 2.2.1.3.2 provides a simplified method of predicting the equiprobable rain attenuation at frequency f_2 conditioned on the rain attenuation at frequency f_1. This method does not require the cumulative distribution of the rain attenuation at either frequency.

These prediction methods may be applicable to uplink power control and adaptive coding and modulation, for example:

a) The first method predicts the instantaneous uplink rain attenuation at frequency f_2 based on the measured instantaneous downlink rain attenuation at frequency f_1 for a p% risk the actual uplink rain attenuation will exceed the predicted value.

b) The second method predicts the uplink rain attenuation at frequency f_2 based on knowledge of the downlink rain attenuation at frequency f_1 at the same probability of exceedance.

2.2.1.3.1 Conditional distribution of the frequency scaling ratio of rain attenuation

This prediction method is based on the following relation between A_2 (dB), the instantaneous rain attenuation at frequency f_2, and A_1 (dB), the instantaneous rain attenuation at frequency f_1.

$$\ln(A_2) = \frac{\sigma_2}{\sigma_1}\sqrt{1-\xi^2}\,\ln(A_1) + \left(\mu_2 - \frac{\sigma_2\mu_1}{\sigma_1}\sqrt{1-\xi^2}\right) + \sigma_2\xi \times n \tag{15}$$

where n is a normal distribution with zero mean and unit variance. The following step-by-step procedure predicts $P(A_2 > a_2 | A_1 = a_1)$, the complementary cumulative distribution function of the rain attenuation at frequency f_2 conditioned on the rain attenuation at frequency f_1.

This method assumes $P(A_1 > a_1 | A_1 > 0)$ and $P(A_2 > a_2 | A_2 > 0)$, the complementary cumulative distributions of rain attenuation conditioned on the occurrence of non-zero rain attenuation on the path at frequencies f_1 and f_2 are characterized by log-normal distributions with parameters (μ_1, σ_1) and (μ_2, σ_2):

$$P(A_1 > a_1 | A_1 > 0) = Q\left(\frac{\ln a_1 - \mu_1}{\sigma_1}\right) \tag{16a}$$

$$P(A_2 > a_2 | A_2 > 0) = Q\left(\frac{\ln a_2 - \mu_2}{\sigma_2}\right) \tag{16b}$$

where:

$$Q(x) = \frac{1}{\sqrt{2\pi}}\int_x^\infty \mathrm{e}^{-\frac{t^2}{2}}\,\mathrm{d}t \tag{17}$$

The parameters μ_1, σ_1, μ_2 and σ_2 are derived from the rain attenuation statistics at frequencies f_1 and f_2 for the same propagation path. These rain attenuation statistics can be computed from the local measured rain attenuation (i.e. excess attenuation in addition to gaseous attenuation, cloud attenuation, and scintillation fading) data or from the rain attenuation prediction method in § 2.2.1.1 for the specific location and path elevation angle of interest. The rain attenuation statistics at frequencies f_1 and f_2 should be derived from the same source.

The procedure has been tested at frequencies between 19 and 50 GHz, but is recommended for frequencies up to 55 GHz.

The following parameters are required:

f_1: lower frequency at which the rain attenuation is known (GHz)

f_2: higher frequency at which the rain attenuation is predicted (GHz)

P_{rain}: probability of rain (%)

μ_1: mean of the log-normal distribution of rain attenuation at frequency f_1

μ_2: mean of the log-normal distribution of rain attenuation at frequency f_2

σ_1: standard deviation of the log-normal distribution of rain attenuation at frequency f_1

σ_2: standard deviation of the log-normal distribution of rain attenuation at frequency f_2.

For each frequency, f_1 and f_2, perform a log-normal fit to the rain attenuation vs. probability of occurrence as follows:

Step 1: Calculate P_{rain} (%), the time percentage of rain on the path. P_{rain} can be predicted by P_0 (*Lat*, *Lon*) from Recommendation ITU-R P.837 for the latitude and longitude of the location of interest.

Step 2: For f_i, where i = 1 and 2, construct the sets of pairs [P_i, $A_{i,1}$] and [P_i, $A_{i,2}$] where P_i (%) is the time percentage the attenuation $A_{i,1}$ (dB) is exceeded, where $P_i \leq P_{rain}$. The specific values of P_i should be selected to encompass the probability range of interest; however, a suggested set of time percentages is 0.01, 0.02, 0.03, 0.05, 0.1, 0.2, 0.3, 0.5, 1, 2, 3 and 5%, with the constraint that $P_i \leq P_{rain}$.

Step 3: Divide all time percentages, P_i, by the probability of rain, P_{rain}, to obtain the conditional rain attenuation probabilities $p_i = P_i / P_{rain}$.

Step 4: Transform the two sequences of pairs [p_i, $A_{i,1}$] and [p_i, $A_{i,2}$] to $\left[Q^{-1}(p_i), \ln A_{i,1}\right]$ and $\left[Q^{-1}(p_i), \ln A_{i,2}\right]$.

Step 5: Estimate the parameters μ_1, σ_1, μ_2 and σ_2 by performing a least-square fit of the two sequences to $\ln A_{i,1} = \sigma_1 Q^{-1}(p_i) + \mu_1$ and $\ln A_{i,2} = \sigma_2 Q^{-1}(p_i) + \mu_2$. Refer to Annex 2 of Recommendation ITU-R P.1057 for a description of a step-by-step procedure to approximate a complementary cumulative distribution by a log-normal complementary cumulative distribution.

Step 6: Calculate the frequency dependency factor, ξ:

$$\xi = 0.19\left[\frac{f_2}{f_1} - 1\right]^{0.57} \tag{18}$$

Step 7: Calculate the conditional mean, $\mu_{2/1}$, and the conditional standard deviation, $\sigma_{2/1}$ as follows:

$$\mu_{2/1} = \frac{\sigma_2}{\sigma_1}\sqrt{1-\xi^2}\,\ln(a_1) + \left(\mu_2 - \frac{\sigma_2 \mu_1}{\sigma_1}\sqrt{1-\xi^2}\right) \tag{19}$$

$$\sigma_{2/1} = \sigma_2 \xi \tag{20}$$

Then $P(A_2 > a_2 | A_1 = a_1)$, the complementary cumulative distribution of rain attenuation A_2 at frequency f_2 conditioned on the rain attenuation $A_1 = a$ at frequency f_1, is:

$$P\left(A_2 > a_2 \middle| A_1 = a_1\right) = Q\left(\frac{\ln(a_2) - \mu_{2/1}}{\sigma_{2/1}}\right) \tag{21}$$

where a_1 (dB) is the rain attenuation at frequency f_1, and $0 \leq P \leq 1$. $P\left(A_2 > a_2 \middle| A_1 = a_1\right)$ represents the probability that the rain attenuation A_2 (dB) at frequency f_2 exceeds a_2 (dB) (i.e. the risk) given the rain attenuation is a_1 (dB) at frequency f_1.

The value of a_2 (dB) can be calculated for an assumed value of P as follows:

$$a_2 = \exp(\sigma_{2/1} Q^{-1}(P) + \mu_{2/1}) \tag{22}$$

While this procedure was derived for the rain attenuation, it can be also used to predict the complementary cumulative distribution of the total attenuation (gaseous attenuation, rain attenuation, cloud attenuation, and scintillation fading). However, the accuracy of this procedure has not been established.

2.2.1.3.2 Long-term frequency scaling of rain attenuation statistics

If reliable attenuation data measured at one frequency are available, the following empirical formula giving an attenuation ratio directly as a function of frequency and attenuation may be applied for frequency scaling on the same path in the frequency range 7 to 55 GHz:

$$A_2 = A_1 (\varphi_2 / \varphi_1)^{1 - H(\varphi_1, \varphi_2, A_1)} \tag{23}$$

where:

$$\varphi(f) = \frac{f^2}{1 + 10^{-4} f^2} \tag{24a}$$

$$H(\varphi_1, \varphi_2, A_1) = 1.12 \times 10^{-3} (\varphi_2 / \varphi_1)^{0.5} (\varphi_1 A_1)^{0.55} \tag{24b}$$

A_1 and A_2 are the equiprobable values of the excess rain attenuation at frequencies f_1 and f_2 (GHz), respectively.

Frequency scaling of attenuation from reliable long-term measured attenuation data, rather than long-term measured rain data, is preferred.

2.2.2 Seasonal variations – worst month

System planning often requires the attenuation value exceeded for a time percentage, p_w, of the worst month. The following procedure is used to estimate the attenuation exceeded for a specified percentage of the worst month.

Step 1: Obtain the annual time percentage, p, corresponding to the desired worst-month time percentage, p_w, by using the equation specified in Recommendation ITU-R P.841 and by applying any adjustments to p as prescribed therein.

Step 2: For the path in question obtain the attenuation, A (dB), exceeded for the resulting annual time percentage, p, from the method of § 2.2.1.1, or from measured or frequency-scaled attenuation statistics. This value of A is the estimated attenuation for p_w per cent of the worst month.

Curves giving the variation of worst-month values from their mean are provided in Recommendation ITU-R P.678.

2.2.3 Variability in space and time of statistics

Precipitation attenuation distributions measured on the same path at the same frequency and polarization may show marked year-to-year variations. In the range 0.001% to 0.1% of the year, the

attenuation values at a fixed probability level are observed to vary by more than 20% r.m.s. When the models for attenuation prediction or scaling in § 2.2.1 are used to scale observations at a location to estimate for another path at the same location, the variations increase to more than 25% r.m.s.

2.2.4 Site diversity

Intense rain cells that cause large attenuation values on an Earth-space link often have horizontal dimensions of no more than a few kilometres. Diversity systems able to re-route traffic to alternate earth stations, or with access to a satellite with extra on-board resources available for temporary allocation, can improve the system reliability considerably. Site diversity systems are classified as balanced if the attenuation thresholds on the two links are equal, and unbalanced if the attenuation thresholds on the two links are not equal. At frequencies above 20 GHz, path impairments other than rain can also affect site diversity performance.

There are two site diversity predictions models:

– the prediction method described in § 2.2.4.1 that is applicable to unbalanced and balanced systems and computes the joint probability of exceeding attenuation thresholds; and

– the prediction method described in § 2.2.4.2 that is applicable to balanced systems with short distances and computes the diversity gain.

The prediction method described in § 2.2.4.1 is the most accurate and is preferred. The simplified prediction method described in § 2.2.4.2 may be used for separation distances less than 20 km; however, it is less accurate.

2.2.4.1 Prediction of outage probability due to rain attenuation with site diversity

The diversity prediction method assumes a log-normal distribution of rain intensity and rain attenuation.

This method predicts $P_r\,(A_1 \geq a_1, A_2 \geq a_2)$, the joint probability (%) that the attenuation on the path to the first site is greater than a_1 and the attenuation on the path to the second site is greater than a_2. $P_r\,(A_1 \geq a_1, A_2 \geq a_2)$ is the product of two joint probabilities:

1) P_r, the joint probability that it is raining at both sites; and

2) P_a, the conditional joint probability that the attenuations exceed a_1 and a_2, respectively, given that it is raining at both sites; i.e.:

$$P_r\,(A_1 \geq a_1, A_2 \geq a_2) = 100 \times P_r \times P_a\% \tag{25}$$

These probabilities are:

$$P_r = \frac{1}{2\pi\sqrt{1-\rho_r^2}} \int_{R_1}^{\infty} \int_{R_2}^{\infty} \exp\left[-\left(\frac{r_1^2 - 2\rho_r r_1 r_2 + r_2^2}{2\left(1-\rho_r^2\right)}\right)\right] \mathrm{d}r_2 \mathrm{d}r_1 \tag{26}$$

where:

$$\rho_r = 0.7\exp\left(-d/60\right) + 0.3\exp\left[-\left(d/700\right)^2\right] \tag{27}$$

and

$$P_a = \frac{1}{2\pi\sqrt{1-\rho_a^2}} \int_{\frac{\ln a_1 - m_{\ln A_1}}{\sigma_{\ln A_1}}}^{\infty} \int_{\frac{\ln a_2 - m_{\ln A_2}}{\sigma_{\ln A_2}}}^{\infty} \exp\left[-\left(\frac{b_1^2 - 2\rho_a b_1 b_2 + b_2^2}{2\left(1-\rho_a^2\right)}\right)\right] db_2 \mathrm{d}b_1 \tag{28}$$

where:

$$\rho_a = 0.94 \exp\left(-d/30\right) + 0.06 \exp\left[-\left(d/500\right)^2\right] \quad (29)$$

and P_a and P_r are complementary bivariate normal distributions[2].

The parameter d is the separation between the two sites (km). The thresholds R_1 and R_2 are the solutions of:

$$P_k^{rain} = 100 \times Q(R_k) = 100 \times \frac{1}{\sqrt{2\pi}} \int_{R_k}^{\infty} \exp\left(-\frac{r^2}{2}\right) dr \quad (30)$$

i.e.:

$$R_k = Q^{-1}\left(\frac{P_k^{rain}}{100}\right) \quad (31)$$

where:

R_k: threshold for the k-th site, respectively

P_k^{rain}: probability of rain (%)

Q: complementary cumulative normal distribution

Q^{-1}: inverse complementary cumulative normal distribution

P_k^{rain}: for a particular location can be obtained from Step 3 of Annex 1 of Recommendation ITU-R P.837 using either local data or the ITU-R rainfall rate maps.

The values of the parameters $m_{\ln A_1}$, $m_{\ln A_2}$, $\sigma_{\ln A_1}$, and $\sigma_{\ln A_2}$ are determined by fitting each single-site rain attenuation, A_i, vs. probability of occurrence, P_i, to the log-normal distribution:

$$P_i = P_k^{rain} Q\left(\frac{\ln A_i - m_{\ln A_i}}{\sigma_{\ln A_i}}\right) \quad (32)$$

These parameters can be obtained for each individual location, or a single location can be used. The rain attenuation vs. annual probability of occurrence can be predicted using the method described in § 2.2.1.1.

For each path, the log-normal fit of rain attenuation vs. probability of occurrence is performed as follows:

Step 1: Determine P_k^{rain} (% of time), the probability of rain on the k-th path.

---

[2] NOTE – This is the same bivariate normal integral used in § 2.2.1.2. An approximation to this integral is available in Z. Drezner and G.O. Wesolowsky. "On the Computation of the Bivariate Normal Integral", Journal of Statistical Computation and Simulation. Vol. 35, 1989, pp. 101–107. The Matlab statistics toolbox contains the built-in Matlab function '*mvncdf*' that computes the bivariate normal integral, and the Python library contains the built-in function 'mvndst' that computes the bivariate normal integral.

Step 2: Construct the set of pairs [P_i, A_i] where P_i (% of time) is the probability the attenuation A_i (dB) is exceeded where $P_i \le P_k^{rain}$. The specific values of P_i should consider the probability range of interest; however, a suggested set of time percentages is 0.01%, 0.02%, 0.03%, 0.05%, 0.1%, 0.2%, 0.3%, 0.5%, 1%, 2%, 3%, 5% and 10%, with the constraint that $P_i \le P_k^{rain}$.

Step 3: Transform the set of pairs [P_i, A_i] to $\left[Q^{-1}\left(\frac{P_i}{P_k^{rain}} \right), \ln A_i \right]$ (33)

where:

$$Q(x) = \frac{1}{\sqrt{2\pi}} \int_x^\infty e^{-\frac{t^2}{2}} dt \tag{34}$$

Step 4: Determine the variables $m_{\ln A_i}$ and $\sigma_{\ln A_i}$ by performing a least-squares fit to: $\ln A_i = \sigma_{\ln A_i} \; Q^{-1}\left(\frac{P_i}{P_k^{rain}} \right) + m_{\ln A_i}$ for all i. The least-squares fit can be determined using the step-by-step procedure to approximate a complementary cumulative distribution by a log-normal complementary cumulative distribution described in Recommendation ITU-R P.1057.

2.2.4.2 Diversity gain

While the prediction method described in § 2.2.4.1 is preferred, an alternate simplified method to predict the diversity gain, G (dB), between pairs of sites can be calculated with the empirical expression given below. This alternate method can be used for site separations of less than 20 km. Parameters required for the calculation of diversity gain are:

d: separation (km) between the two sites

A: path rain attenuation (dB) for a single site

f: frequency (GHz)

θ: path elevation angle (degrees)

ψ: angle (degrees) made by the azimuth of the propagation path with respect to the baseline between sites, chosen such that $\psi \le 90°$.

Step 1: Calculate the gain contributed by the spatial separation from:

$$G_d = a \left(1 - e^{-bd}\right) \tag{35}$$

where:

$$a = 0.78\, A - 1.94 \left(1 - e^{-0.11\, A}\right)$$

$$b = 0.59 \left(1 - e^{-0.1\, A}\right)$$

Step 2: Calculate the frequency-dependent gain from:

$$G_f = e^{-0.025\, f} \tag{36}$$

Step 3: Calculate the gain term dependent on elevation angle from:

$$G_\theta = 1 + 0.006\, \theta \tag{37}$$

Step 4: Calculate the baseline-dependent term from the expression:

$$G_\psi = 1 + 0.002\ \psi \tag{38}$$

Step 5: Compute the net diversity gain as the product:

$$G = G_d \cdot G_f \cdot G_\theta \cdot G_\psi \quad \text{dB} \tag{39}$$

2.2.5 Characteristics of precipitation events

2.2.5.1 Durations of individual fades

The durations of rain fades that exceed a specified attenuation level are approximately log-normally distributed. Median durations are of the order of several minutes. No significant dependence of these distributions on fade depth is evident in most measurements for fades of less than 20 dB, implying that the larger total time percentage of fades observed at lower fade levels or at higher frequencies is composed of a larger number of individual fades having more or less the same distribution of durations. Significant departures from log-normal seem to occur for fade durations of less than about half a minute. Fade durations at a specified fade level tend to increase with decreasing elevation angle.

For the planning of integrated services digital network (ISDN) connections via satellite, data are needed on the contribution of attenuation events shorter than 10 s to the total fading time. This information is especially relevant for the attenuation level corresponding to the outage threshold, where events longer than 10 s contribute to system unavailable time, while shorter events affect system performance during available time (see Recommendation ITU-R S.579). Existing data indicate that in the majority of cases, the exceedance time during available time is 2% to 10% of the net exceedance time. However, at low elevation angles where the short period signal fluctuations due to tropospheric scintillation become statistically significant, there are some cases for which the exceedance time during available time is far larger than in the case at higher elevation Earth-space paths.

2.2.5.2 Rates of change of attenuation (fading rate)

There is broad agreement that the distributions of positive and negative fade rates are log-normally distributed and very similar to each other. The dependence of fade rate on fade depth has not been established.

2.2.5.3 Correlation of instantaneous values of attenuation at different frequencies

Data on the instantaneous ratio of rain attenuation values at different frequencies are of interest for a variety of adaptive fade techniques. The frequency-scaling ratio has been found to be log-normally distributed, and is influenced by rain type and rain temperature. Data reveal that the short-term variations in the attenuation ratio can be significant, and are expected to increase with decreasing path elevation angle.

2.3 Clear-air effects

Other than atmospheric absorption, clear-air effects in the absence of precipitation are unlikely to produce serious fading in space telecommunication systems operating at frequencies below about 10 GHz and at elevation angles above 10°. At low elevation angles ($\leq 10°$) and at frequencies above about 10 GHz, however, tropospheric scintillations can on occasion cause serious degradations in performance. At very low elevation angles ($\leq 4°$ on inland paths, and $\leq 5°$ on overwater or coastal paths), fading due to multipath propagation effects can be particularly severe. At some locations, ionospheric scintillation may be important at frequencies below about 6 GHz (see Recommendation ITU-R P.531).

2.3.1 Decrease in antenna gain due to wave-front incoherence

Incoherence of the wave-front of a wave incident on a receiving antenna is caused by small-scale irregularities in the refractive index structure of the atmosphere. Apart from the rapid signal fluctuations discussed in § 2.4, they cause an antenna-to-medium coupling loss that can be described as a decrease of the antenna gain.

This effect increases both with increasing frequency and decreasing elevation angle, and is a function of antenna diameter. Although not explicitly accounted for in the refraction models presented below, this effect is negligible in comparison.

2.3.2 Beam spreading loss

The regular decrease of refractive index with height causes ray-bending and hence a defocusing effect at low angles of elevation (Recommendation ITU-R P.834). The magnitude of the defocusing loss of the antenna beam is independent of frequency, over the range of 1-100 GHz.

The loss A_{bs} due to beam spreading in regular refractive conditions can be ignored at elevation angles above about 3° at latitudes less than 53° and above about 6° at higher latitudes.

At all latitudes, the beam spreading loss in the average year at elevation angles less than 5° is estimated from:

$$A_{bs} = 2.27 - 1.16 \log (1 + \theta_0) \quad \text{dB} \quad \text{for } A_{bs} > 0 \tag{40}$$

where θ_0 is the apparent elevation angle (mrad) taking into account the effects of refraction. The beam spreading loss in the average worst month at latitudes less than 53° is also estimated from equation (40).

At latitudes greater than 60°, the beam spreading loss at elevation angles less than 6° in the average worst month is estimated from:

$$A_{bs} = 13 - 6.4 \log (1 + \theta_0) \quad \text{dB} \quad \text{for } A_{bs} > 0 \tag{41}$$

At latitudes ψ between 53° and 60°, the median beam spreading loss can be estimated by a linear interpolation between the values obtained from equation (40) (designated A_{bs} (< 53°)) and equation (41) (designated A_{bs} (> 60°)) as follows:

$$A_{bs} = A_{bs}\ (> 60°) - \frac{60}{7} \Delta A_{bs} + \frac{1}{7} \Delta A_{bs}\ \psi \quad \text{dB} \tag{42}$$

where $\Delta A_{bs} = A_{bs}$ (> 60°) – A_{bs} (< 53°).

2.4 Scintillation and multipath fading

The amplitude of tropospheric scintillations depends on the magnitude and structure of the refractive index variations along the propagation path. Amplitude scintillations increase with frequency and with the path length, and decrease as the antenna beamwidth decreases due to aperture averaging. Measured data shows the monthly-averaged r.m.s. fluctuations are well-correlated with the wet term of the radio refractivity, N_{wet}, which depends on the water vapour content of the atmosphere.

There are three parts of the method of predicting the fading due to amplitude scintillation:

1) Prediction of the amplitude scintillation fading at free-space elevation angles ≥ 5° (§ 2.4.1).

2) Prediction of the amplitude scintillation fading for fades ≥ 25 dB (§ 2.4.2).

3) Prediction of the amplitude scintillation in the transition region between the above two distributions (§ 2.4.3).

As noted in Recommendation ITU-R P.834, a radio wave between a station on the surface of the Earth and a space station is bent towards the Earth due to the effect of atmospheric refraction. As a result, the apparent elevation angle, which considers atmospheric refraction, is greater than the free-space elevation angle, which only considers the line-of-sight between the two stations. If the free-space elevation angle of interest is greater than or equal to 5°, the difference between the apparent and free-space elevation angles is insignificant, and only the prediction method described in § 2.4.1 needs to be considered.

An illustrative example of the three parts of the prediction method is shown in Fig. 2. Note that the prediction method in the transition region described in § 2.4.3 is tangent to the distribution described in § 2.4.1 at a free-space elevation angle of 5° and tangent to the distribution described in § 2.4.2 at a scintillation fading depth of 25 dB.

FIGURE 2

Illustrative example of three parts of the scintillation prediction method

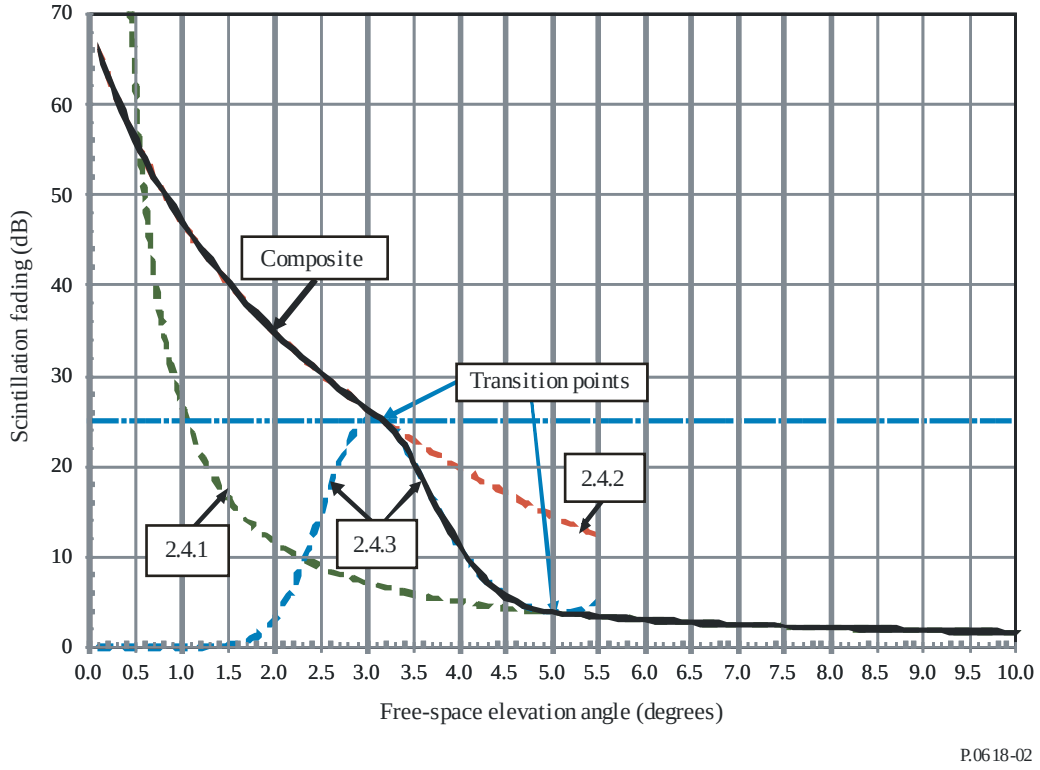

At very small percentages of time, and similarly for large fade depths (greater than about 10 dB), the fading due to scintillation at very low elevation angles can be significant. The fading is also observed to have a character similar to multipath fading on terrestrial links. Similar to the distribution of fade depths on terrestrial links, the distribution of fade depths for very low angle satellite links also appears correlated with refractivity gradient statistics. The overall fading distribution shows a gradual transition from a scintillation distribution at large exceedance percentages to a multipath fading distribution (with a slope of 10 dB/decade) at small percentages. The prediction methods in §§ 2.4.2 and 2.4.3 for the deep fading and shallow fading portions of the overall distribution, respectively, use the refractivity gradient statistic, p_L, to describe the climatic variations in the distribution.

The net fade distribution due to tropospheric refractive effects, $A(p)$, is the combination of beam spreading, scintillation, and multipath-fading effects described above. Tropospheric and ionospheric scintillation distributions may be combined by summing the respective time percentages that specified fade levels are exceeded.

2.4.1 Calculation of monthly and long-term statistics of amplitude scintillations at elevation angles greater than 5°

A general technique for predicting the cumulative distribution of tropospheric scintillation at elevation angles greater than or equal to 5° is given below. It is based on monthly or longer averages of temperature and relative humidity, and reflects the specific climatic conditions of the site. Since the average surface temperature and average surface relative humidity vary with season, the scintillation fade depth distribution varies with season. The seasonal variation may be predicted by using seasonal average surface temperature and seasonal average surface relative humidity. This information may be obtained from weather information for the site of interest.

While the procedure has been tested at frequencies between 7 and 14 GHz, it is recommended for applications up to at least 20 GHz.

The parameters required for the method are:

t: average surface ambient temperature (°C) at the site for a period of one month or longer

H: average surface relative humidity (%) at the site for a period of one month or longer

(NOTE 1 – If no experimental data are available for t and H, the maps of N_{wet} in Recommendation ITU-R P.453 may be used.)

f: frequency (GHz), where 4 GHz $\leq f \leq$ 20 GHz

θ: free-space elevation angle, where $\theta \geq 5°$

D: physical diameter (m) of the earth-station antenna

η: antenna efficiency; if unknown, $\eta = 0.5$ is a conservative estimate.

If the median value of the wet term of the surface refractivity exceeded for the average year, N_{wet}, is obtained from the digital maps in Recommendation ITU-R P.453, go directly to Step 3.

Step 1: For the value of t, calculate the saturation water vapour pressure, e_s, (hPa), as specified in Recommendation ITU-R P.453.

Step 2: Compute the wet term of the radio refractivity, N_{wet}, corresponding to e_s, t and H as given in Recommendation ITU-R P.453.

Step 3: Calculate the standard deviation of the reference signal amplitude, σ_{ref},:

$$\sigma_{ref} = 3.6 \times 10^{-3} + 10^{-4} \times N_{wet} \quad \text{dB} \tag{43}$$

Step 4: Calculate the effective path length L:

$$L = \frac{2h_L}{\sqrt{\sin^2 \theta + 2.35 \times 10^{-4}} + \sin\theta} \quad \text{m} \tag{44}$$

where h_L, the height of the turbulent layer, is 1 000 m.

Step 5: Estimate the effective antenna diameter, D_{eff}, from the geometrical diameter, D, and the antenna efficiency η:

$$D_{eff} = \sqrt{\eta}\, D \quad \text{m} \tag{45}$$

Step 6: Calculate the antenna averaging factor:

$$g(x) = \sqrt{3.86\,(x^2+1)^{11/12} \cdot \sin\left[\frac{11}{6}\tan^{-1}\frac{1}{x}\right] - 7.08\,x^{5/6}} \tag{46}$$

where:

$$x = 1.22\,D_{eff}^2\,(f / L) \tag{46a}$$

If the argument of the square root is negative (i.e. when $x \geq 7.0$), the predicted scintillation fade depth for any time percentage is zero and the following steps are not required.

Step 7: Calculate the standard deviation of the signal for the applicable period and propagation path:

$$\sigma = \sigma_{ref}\; f^{\,7/12}\; \frac{g(x)}{(\sin\theta)^{1.2}} \tag{47}$$

Step 8: Calculate the time percentage factor, $a(p)$, for the time percentage, p, in the range between $0.01\% < p \leq 50\%$:

$$a(p) = -0.061\,(\log_{10} p)^3 + 0.072\,(\log_{10} p)^2 - 1.71\,\log_{10} p + 3.0 \tag{48}$$

Step 9: Calculate the fade depth, $A(p)$, exceeded for p% of the time:

$$A(p) = a(p) \cdot \sigma \qquad \text{dB} \tag{49}$$

2.4.2 Calculation of the deep fading part of the scintillation/multipath fading distribution of elevation angles less than 5°

This method estimates the fade depth for fades greater than or equal to 25 dB due to the combination of beam spreading, scintillation and multipath fading in the average year and average annual worst-month. The step-by-step procedure is as follows:

Step 1: Calculate the apparent boresight elevation angle θ (mrad) corresponding to the desired free-space elevation angle θ_0 (mrad) accounting for the effects of refraction for the path of interest using the method described in § 4 of Recommendation ITU-R P.834.

Step 2: For the path of interest, calculate the geoclimatic factor, K_w, for the average annual worst month:

$$K_w = p_L^{1.5} \times 10^{\frac{C_0 + C_{Lat}}{10}} \tag{50}$$

where p_L (%) is the percentage of time that the refractivity gradient in the lowest 100 m of the atmosphere is less than –100 N units/km in that month having the highest value of p_L from the four seasonally representative months of February, May, August and November for which maps are given in Figures 8 to 11 of Recommendation ITU-R P.453.

As an exception, only the maps for May and August should be used for latitudes greater than 60° N or 60° S.

Values of the coefficient C_0 in equation (50) corresponding to the type of path are summarized in Table 3. The coefficient C_{Lat} vs. latitude ψ (in °N or °S) is given by:

$$C_{Lat} = 0 \qquad \text{for} \qquad |\psi| \leq 53° \tag{51}$$

$$C_{Lat} = -53 + \psi \qquad \text{for} \qquad 53° < |\psi| \leq 60° \tag{52}$$

$$C_{Lat} = 7 \qquad \text{for} \qquad 60° < |\psi| \tag{53}$$

TABLE 3

Values of the coefficient C_0 in equation (50) for various types of propagation path

Type of path	C_0
Propagation paths entirely over land for which the earth-station antenna is less than 700 m above mean sea level	76
Propagation paths for which the earth-station antenna is higher than 700 m above mean sea level	70
Propagation paths entirely or partially over water or coastal areas beside such bodies of water (see[1] for definition of propagation path, coastal areas, and definition of r)	$76 + 6r$

(1) The variable r in the expression for C_0 is the fraction of the propagation path that crosses a body of water or adjacent coastal areas. Propagation paths passing over a small lake or river are classed as being entirely over land. Although such bodies of water could be included in the calculation of r, this yields negligible increases in the value of the coefficient C_0 from the overland non-coastal values.

Step 3: Calculate the fade depth, $A(p)$, exceeded for p% of the time at frequency f (GHz), and the desired apparent elevation angle, θ (mrad)

a) for the average year:

$$A(p) = 10\log_{10} K_w - v + 9\log_{10} f - 59.5\log_{10}(1+\theta) - 10\log_{10} p \quad \text{dB} \tag{54}$$

where:

$$v = -1.8 - 5.6\log_{10}(1.1 \pm |\cos 2\psi|^{0.7}) \quad \text{dB} \tag{55}$$

and the positive sign in equation (55) is for latitudes $|\psi| \leq 45°$, and the negative sign is for latitudes $|\psi| > 45°$;

or

b) for the average annual worst-month:

$$A(p) = 10\log_{10} K_w + 9\log_{10} f - 55\log_{10}(1+\theta) - 10\log_{10} p \quad \text{dB} \tag{56}$$

Equations (54), (55) and (56) are valid for $A(p)$ greater than or equal to 25 dB. These equations were developed from data in the frequency range 6-38 GHz and elevation angles in the range from 1° to 4°. They are expected to be valid at least in the frequency range from 1 to 45 GHz and elevation angles in the range from 0.5° to 5°.

2.4.3 Calculation of the shallow fading part of the scintillation/multipath fading distribution at elevation angles less than 5°

The shallow fading model in this section is developed for scintillation fading in the transition region for fading less than 25 dB and free-space elevation angles less than 5°.

Step 1: Set A_1 = 25 dB and calculate the apparent elevation angle, θ_1, at the desired time percentage, *p(%)*, and frequency, f (GHz):

percentage, *p(%)*, and frequency, *f* (GHz):

$$\theta_1 = \begin{cases} \left(\dfrac{K_w f^{0.9}}{p 10^{\frac{A_1}{10}}} \right)^{\frac{1}{5.5}} - 1 & \text{worst month} \\ \left(\dfrac{K_w 10^{-\frac{\nu}{10}} f^{0.9}}{p 10^{\frac{A_1}{10}}} \right)^{\frac{1}{5.95}} - 1 & \text{average year} \end{cases} \quad \text{mrad} \tag{57}$$

where the geoclimatic factor, K_w, is defined in equation (50), and ν is defined in equation (56).

Step 2: Calculate A_1'

$$A_1' = \begin{cases} -\dfrac{55}{1+\theta_1} \log_{10} e & \text{worst month} \\ -\dfrac{59.5}{1+\theta_1} \log_{10} e & \text{average year} \end{cases} \quad \text{dB/mrad} \tag{58}$$

Step 3: Calculate A_2 from equation (49) of § 2.4.1

$$A_2 = A_s(p) \quad \text{dB} \tag{59}$$

at a free-space elevation angle, θ, of 5°.

Step 4: Calculate A_2' as follows:

$$A_2' = A_2 \times \left[\frac{g'(x)}{g(x)} \frac{dx}{d\theta} - \frac{1.2}{\tan(\theta)} \right] \times \frac{1}{1000} \quad \text{dB/mrad} \tag{60}$$

where:

$$\frac{g'(x)}{g(x)} = \frac{1770\left(x^2+1\right) + 2123 x^{\frac{1}{6}} \left(x^2+1\right)^{\frac{11}{12}} \left[\cos\zeta - x \sin\zeta\right]}{12 x^{\frac{1}{6}} \left(x^2+1\right) \left[354 x^{\frac{5}{6}} - 193 \left(x^2+1\right)^{\frac{11}{12}} \sin\zeta \right]} \tag{61a}$$

$$\frac{dx}{d\theta} = \frac{1.22 D_{eff}^2 f}{2 h_L} \left[\frac{\sin\theta}{\sqrt{\sin^2\theta + 2.35 \times 10^{-4}}} + 1 \right] \cos\theta \tag{61b}$$

and

$$\zeta = \frac{11}{6} \tan^{-1} \frac{1}{x} \tag{61c}$$

at a free-space elevation angle, θ, of 5°, where *x*, D_{eff} and h_L are defined in § 2.4.1.

Step 5: Calculate the apparent elevation angle, θ_2, corresponding to a free-space elevation angle of 5° using equation (12) of Recommendation ITU-R P.834, and convert θ_2 to mrad.

Step 6: Calculate the scintillation fading, $A(p)$, exceeded for p (%) of the time at the desired apparent elevation angle, θ (mrad), by interpolating between the points (θ_1, A_1, A_1') and (θ_2, A_2, A_2') using the following cubic exponential model:

$$A(p) = A_1 \exp\left[\alpha(p)(\theta-\theta_1) + \beta(p)(\theta-\theta_1)^2 + \gamma(p)(\theta-\theta_1)^2(\theta-\theta_2)\right] \quad (62)$$

where:

$$\alpha(p) = \frac{A_1'}{A_1}$$

$$\beta(p) = \frac{\ln\left(\frac{A_2}{A_1}\right) - \alpha\delta}{\delta^2}$$

$$\gamma(p) = \frac{A_2' - A_2(\alpha + 2\beta\delta)}{A_2\delta^2}$$

$$\delta = \theta_2 - \theta_1$$

The fade depth, $A(p)$, is applicable for apparent elevation angles in the transition region; i.e. for $\theta_1 \le \theta \le \theta_2$, and $0 \le p \le 50\%$.

2.5 Estimation of total attenuation due to multiple sources of simultaneously occurring atmospheric attenuation

For systems operating at frequencies above about 18 GHz, and especially those operating with low elevation angles and/or margins, the effect of multiple sources of simultaneously occurring atmospheric attenuation must be considered.

Total attenuation (dB) represents the combined effect of rain, gas, clouds and scintillation and requires one or more of the following input parameters:

$A_R(p)$: attenuation due to rain for a fixed probability (dB), as estimated by A_p in equation (8)

$A_C(p)$: attenuation due to clouds for a fixed probability (dB), as estimated by Recommendation ITU-R P.840

$A_G(p)$: gaseous attenuation due to water vapour and oxygen for a fixed probability (dB), as estimated by Recommendation ITU-R P.676

$A_S(p)$: attenuation due to tropospheric scintillation for a fixed probability (dB), as estimated by equation (49)

where p is the probability of the attenuation being exceeded in the range 50% to 0.001%.

Gaseous attenuation as a function of percentage of time can be calculated using § 2.2 of Annex 2 of Recommendation ITU-R P.676 if local meteorological data at the required time percentage are available. In the absence of local data at the required time percentage, the mean gaseous attenuation should be calculated and used in equation (63).

A general method for calculating total attenuation for a given probability, $A_T(p)$, is given by:

$$A_T(p) = A_G(p) + \sqrt{\left(A_R(p) + A_C(p)\right)^2 + A_S^2(p)} \quad (63)$$

where:

$$A_C(p) = A_C(1\%) \qquad \text{for } p < 1.0\% \tag{64}$$

$$A_G(p) = A_G(1\%) \qquad \text{for } p < 1.0\% \tag{65}$$

Equations (64) and (65) take account of the fact that a large part of the cloud attenuation and gaseous attenuation is already included in the rain attenuation prediction for time percentages below 1%.

When the complete prediction method above was tested using the procedure set out in Annex 1 to Recommendation ITU-R P.311, the results were found to be in good agreement with available measurement data for all latitudes and in the probability range 0.001% to 1%, with an overall r.m.s. error of about 35%, when used with the contour rain maps in Recommendation ITU-R P.837. When tested against multi-year Earth-space data, the overall r.m.s. error was found to be about 25%. Due to the dominance of different effects at different probabilities as well as the inconsistent availability of test data at different probability levels, some variation of r.m.s. error occurs across the distribution of probabilities.

2.6 Attenuation by sand and dust storms

Very little is known about the effects of sand and dust storms on radio signals on slant-paths. Available data indicate that at frequencies below 30 GHz, high particle concentrations and/or high moisture contents are required to produce significant propagation effects.

3 Noise temperature

As attenuation increases, so does emission noise. For earth stations with low-noise front-ends, this increase of noise temperature may have a greater impact on the resulting signal-to-noise ratio than the attenuation itself.

The sky noise temperature at a ground station antenna may be estimated by:

$$T_{sky} = T_{mr}\,(1 - 10^{-A/10}) + 2.7 \times 10^{-A/10} \quad \text{K} \tag{66}$$

where:

T_{sky} : sky noise temperature (K) at the ground station antenna

A : total atmospheric attenuation excluding scintillation fading (dB)

T_{mr} : atmospheric mean radiating temperature (K).

When the surface temperature T_s (K) is known, the mean radiating temperature, T_{mr}, may be estimated for clear and cloudy weather as:

$$T_{mr} = 37.34 + 0.81 \times T_S \quad \text{K} \tag{67}$$

In the absence of local data, an atmospheric mean radiating temperature, T_{mr}, of 275 K may be used for clear and rainy weather.

The noise environments of stations on the surface of the Earth and in space are treated in detail in Recommendation ITU-R P.372.

For satellite telecommunication systems using the geostationary orbit, earth stations will find that the Sun and, to a lesser extent, the Moon, are significant noise sources at all frequencies, and the galactic background is a possibly significant consideration at frequencies below about 2 GHz (see Recommendation ITU-R P.372). In addition, Cygnus A and X, Cassiopeia A, Taurus and the Crab nebula may contribute to the sky background noise temperature.

Refer to Recommendation ITU-R P.372 to determine the earth station system noise temperature from the brightness temperatures discussed above.

4 Cross-polarization effects

Frequency reuse by means of orthogonal polarizations is often used to increase the capacity of space telecommunication systems. This technique is restricted, however, by depolarization on atmospheric propagation paths. Various depolarization mechanisms, especially hydrometeor effects, are important in the troposphere.

Faraday rotation of the plane of polarization by the ionosphere is discussed in Recommendation ITU-R P.531. As much as 1° of rotation may be encountered at 10 GHz, and greater rotations at lower frequencies. As seen from the earth station, the planes of polarization rotate in the same direction on the up- and down-links. It is therefore not possible to compensate for Faraday rotation by rotating the feed system of the antenna, if the same antenna is used both for transmitting and receiving.

4.1 Calculation of long-term statistics of hydrometeor-induced cross-polarization

To calculate long-term statistics of depolarization from rain attenuation statistics the following parameters are needed:

A_p: rain attenuation (dB) exceeded for the required percentage of time, p, for the path in question, commonly called co-polar attenuation (CPA)

τ: tilt angle of the linearly polarized electric field vector with respect to the horizontal (for circular polarization use $\tau = 45°$)

f: frequency (GHz)

θ: path elevation angle (degrees).

The method described below to calculate cross-polarization discrimination (XPD) statistics from rain attenuation statistics for the same path is valid for $6 \le f \le 55$ GHz and $\theta \le 60°$. The procedure for scaling to frequencies down to 4 GHz is given in § 4.3 (and see Step 8 below).

Step 1: Calculate the frequency-dependent term:

$$C_f = \begin{cases} 60 \log f - 28.3 & 6 \le f < 9 \text{ GHz} \\ 26 \log f + 4.1 & 9 \le f < 36 \text{ GHz} \\ 35.9 \log f - 11.3 & 36 \le f \le 55 \text{ GHz} \end{cases} \quad (68)$$

Step 2: Calculate the rain attenuation dependent term:

$$C_A = V(f) \log A_p \quad (69)$$

where:

$$V(f) = \begin{cases} 30.8 f^{-0.21} & 6 \le f < 9 \text{ GHz} \\ 12.8 f^{0.19} & 9 \le f < 20 \text{ GHz} \\ 22.6 & 20 \le f < 40 \text{ GHz} \\ 13.0 f^{0.15} & 40 \le f \le 55 \text{ GHz} \end{cases}$$

Step 3: Calculate the polarization improvement factor:

$$C_\tau = -10 \log [1 - 0.484 (1 + \cos 4\tau)] \quad (70)$$

The improvement factor $C_\tau = 0$ for $\tau = 45°$ and reaches a maximum value of 15 dB for $\tau = 0°$ or 90°.

Step 4: Calculate the elevation angle-dependent term:

$$C_\theta = -40 \log (\cos \theta) \qquad \text{for } \theta \le 60° \tag{71}$$

Step 5: Calculate the canting angle dependent term:

$$C_\sigma = 0.0053\ \sigma^2 \tag{72}$$

σ is the effective standard deviation of the raindrop canting angle distribution, expressed in degrees; σ takes the value 0°, 5°, 10° and 15° for 1%, 0.1%, 0.01% and 0.001% of the time, respectively.

Step 6: Calculate rain XPD not exceeded for p% of the time:

$$XPD_{rain} = C_f - C_A + C_\tau + C_\theta + C_\sigma \qquad \text{dB} \tag{73}$$

Step 7: Calculate the ice crystal dependent term:

$$C_{ice} = XPD_{rain} \times (0.3 + 0.1 \log p)/2 \qquad \text{dB} \tag{74}$$

Step 8: Calculate the XPD not exceeded for p% of the time, including the effects of ice:

$$XPD_p = XPD_{rain} - C_{ice} \qquad \text{dB} \tag{75}$$

In this prediction method in the frequency band 4 to 6 GHz where path attenuation is low, A_p statistics are not very useful for predicting XPD statistics. For frequencies below 6 GHz, the frequency-scaling formula of § 4.3 can be used to scale cross-polarization statistics calculated for 6 GHz to a lower frequency between 4 and 6 GHz.

4.2 Joint statistics of XPD and attenuation

The conditional probability distribution of XPD for a given value of attenuation, A_p, can be modelled by assuming that the cross-polar to co-polar voltage ratio, $r = 10^{-XPD/20}$, is normally distributed. Parameters of the distribution are the mean value, r_m, which is very close to $10^{-XPD_{rain}/20}$, with XPD_{rain} given by equation (73), and the standard deviation, σ_r, which assumes the almost-constant value of 0.038 for 3 dB $\le A_p \le$ 8 dB.

4.3 Long-term frequency and polarization scaling of statistics of hydrometeor-induced cross-polarization

Long-term XPD statistics obtained at one frequency and polarization tilt angle can be scaled to another frequency and polarization tilt angle using the semi-empirical formula:

$$XPD_2 = XPD_1 - 20 \log \left[\frac{f_2 \sqrt{1 - 0.484\ (1 + \cos 4\ \tau_2)}}{f_1 \sqrt{1 - 0.484\ (1 + \cos 4\ \tau_1)}} \right] \qquad \text{for } 4 \le f_1, f_2 \le 30 \text{ GHz} \tag{76}$$

where XPD_1 and XPD_2 are the XPD values not exceeded for the same percentage of time at frequencies f_1 and f_2 and polarization tilt angles, τ_1 and τ_2, respectively.

Equation (76) is based on the same theoretical formulation as the prediction method of § 4.1, and can be used to scale XPD data that include the effects of both rain and ice depolarization, since it has been observed that both phenomena have approximately the same frequency dependence at frequencies less than about 30 GHz.

4.4 Data relevant to cross-polarization cancellation

Experiments have shown that a strong correlation exists between rain depolarization at 6 and 4 GHz on Earth-space paths, both on the long term and on an event basis, and uplink depolarization compensation utilizing concurrent down-link depolarization measurements appears feasible. Only differential phase effects were apparent, even for severe rain events, and single-parameter compensation (i.e. for differential phase) appears sufficient at 6 and 4 GHz.

Measurements at 6 and 4 GHz have also shown that 99% of the XPD variations are slower than ± 4 dB/s, or equivalently, less than $\pm 1.5°$/s in the mean path differential phase shift. Therefore, the time constant of a depolarization compensation system at these frequencies need only be about 1 s.

5 Propagation delays

Radiometeorologically-based methods for estimating the average propagation delay or range error, and the corresponding variations, for Earth-space paths through the troposphere are available in Recommendation ITU-R P.834. The delay variance is required for satellite ranging and synchronization in digital satellite communication systems. At frequencies above 10 GHz, the ionospheric time delay (see Recommendation ITU-R P.531) is generally smaller than that for the troposphere, but may have to be considered in special cases.

Range determination to centimetre accuracy requires careful consideration of the various contributions to excess range delay. The water vapour component amounts to 10 cm for a zenith path and a reference atmosphere with surface water vapour concentration of 7.5 g/m^3 and 2 km scale height (see Recommendation ITU-R P.676). This contribution is the largest source of uncertainty, even though the dry atmosphere adds 2.3 m of the zenithal excess range delay.

For current satellite telecommunication applications, additional propagation delays contributed by precipitation are sufficiently small to be ignored.

6 Bandwidth limitations

In the vicinity of the absorption lines of atmospheric gases, anomalous dispersion produces small changes in the refractive index. However, these refractive index changes are small in the bands allocated to Earth-space communications, and will not restrict the bandwidth of systems.

Multiple scattering in rain can limit the bandwidth of incoherent transmission systems due to variation in time delays of the multiple-scattered signals; however, the attenuation itself under such circumstances will present a far more serious problem. A study of the problem of bandwidth limitations imposed by the frequency dependence of attenuation and phase shift due to rain on coherent transmission systems showed that such bandwidth limitations are in excess of 3.5 GHz for all situations likely to be encountered. These are greater than any bandwidth allocated for Earth-space communications below 40 GHz, and the rain attenuation will therefore be far more important than its frequency dependence.

7 Angle of arrival

Elevation-angle errors due to refraction are discussed in Recommendation ITU-R P.834. The total angular refraction (the increase in apparent elevation) is about 0.65°, 0.35° and 0.25°, for elevation angles of 1°, 3° and 5°, respectively, for a tropical maritime atmosphere. For a polar continental climate the corresponding values are 0.44°, 0.25° and 0.17°. Other climates will have values between these two extremes. The day-to-day variation in apparent elevation is of the order of 0.1° (r.m.s.) at 1° elevation, but the variation decreases rapidly with increasing elevation angle.

Short-term angle-of-arrival fluctuations are discussed in Recommendation ITU-R P.834. Short-term variations, due to changes in the refractivity-height variation, may be of the order of 0.02° (r.m.s.) at 1° elevation, again decreasing rapidly with increasing elevation angle. In practice, it is difficult to distinguish between the effect of the short-term changes in the refractivity-height distribution and the effect of random irregularities superimposed on that distribution. A statistical analysis of the short-term angle-of-arrival fluctuation at 19.5 GHz and at an elevation angle of 48° suggests that both in elevation and azimuth directions, standard deviations of angle-of-arrival fluctuations are about 0.002° at the cumulative time percentage of 1%. The seasonal variation of angle-of-arrival fluctuations suggests that the fluctuations increase in summer and decrease in winter. The diurnal variation suggests that they increase in the daytime and decrease both in the early morning and the evening.

8 Calculation of long-term statistics for non-GSO paths

The prediction methods described above were derived for applications where the elevation angle remains constant. For non-GSO systems, where the elevation angle is varying, the link availability for a single satellite can be calculated in the following way:

a) calculate the minimum and maximum elevation angles at which the system will be expected to operate;

b) divide the operational range of angles into small increments (e.g. 5° wide);

c) calculate the percentage of time that the satellite is visible as a function of elevation angle in each increment;

d) for a given propagation impairment level, find the time percentage that the level is exceeded for each elevation angle increment;

e) for each elevation angle increment, multiply the results of c) and d) and divide by 100, giving the time percentage that the impairment level is exceeded at this elevation angle;

f) sum the time percentage values obtained in e) to arrive at the total system time percentage that the impairment level is exceeded.

In the case of multi-visibility satellite constellations employing satellite path diversity (i.e. switching to the least impaired path), an approximate calculation can be made assuming that the spacecraft with the highest elevation angle is being used.

_____